

Theoretical Study of the Antioxidant Activity of Vitamin E: Reactions of α -Tocopherol with the Hydroperoxy Radical

Marta Navarrete, Cipriano Rangel, Joaquín Espinosa-García, and José C. Corchado*

Departamento de Química Física, Universidad de Extremadura, 06071 Badajoz, Spain

Received November 9, 2004

Abstract: The reactivity of the hydroperoxy radical with α -tocopherol—a prototype of the chemical reactions involved in biological antioxidant actions—was studied theoretically. Two pathways were analyzed: hydrogen abstraction from the phenolic hydrogen and hydroperoxy addition to the aromatic ring. The reaction paths for the two mechanisms were traced independently, and the respective thermal rate constants were calculated using variational transition-state theory with multidimensional small-curvature tunneling. The reactivity of the hydroperoxy radical was found to be dominated by the hydrogen abstraction mechanism on α -tocopherol, with a rate constant of $1.5 \times 10^5 \text{ M}^{-1} \text{ s}^{-1}$ at 298 K. It was also found that the mechanism of the reaction is not direct but passes through two intermediates, one of which may have a significant role in preventing the pro-oxidant effects of α -tocopherol.

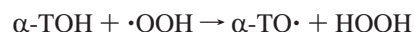
1. Introduction

Vitamin E is the most important lipid-soluble peroxy radical trapping antioxidant, retarding the oxidative degradation of lipids,^{1,2} being located in the lipophilic domains of membranes and lipoproteins.³ Its role is to react with the peroxy radicals present in the cytosol, preventing the chain reactions that lead to lipid peroxidation of the lipidic parts of membranes and lipoproteins.^{3,4} The most active form of vitamin E is α -tocopherol (α -TOH).

Considerable experimental work has been devoted to the study of the activity of free-radical-chain-breaking antioxidants on biological systems.^{2,5,6} α -TOH and coenzyme Q (CoQ) partition in the lipid bilayer and act as natural radical-trapping antioxidants, avoiding or at least significantly reducing free radical reaction damage in the cytosol.^{7–10} From these studies it can be concluded that the antioxidant activity of α -tocopherol depends largely on its location. Thus, its scavenging activity is more pronounced in solution than in membranes and micelle systems,^{11–13} and, when in solution, it significantly depends on the solvent.¹⁴ This dependence has been partially ascribed to the possibility of hydrogen bonding with the solvent.¹⁴ It has been found that the relative antioxidant activities of α -tocopherol versus coenzyme Q

are as follows: $\text{CoQ} > \alpha\text{-TOH}$ in LDL; $\text{CoQ} < \alpha\text{-TOH}$ in homogeneous solution; and $\text{CoQ} \approx \alpha\text{-TOH}$ in aqueous lipid dispersions.¹⁵

It is also well-known that α -tocopherol can act as a pro-oxidant molecule.⁶ This is a result of the relatively long life of the α -tocopheryl radical ($\alpha\text{-TO}\cdot$) formed after the proton-transfer reaction



takes place. This α -tocopheryl radical can react with lipids present in the nearest environment (membranes or lipoproteins) rather than reacting with other molecules that would regenerate the α -tocopherol, such as vitamin C or CoQ. Fortunately, the rate of the hydrogen abstraction reaction from lipids is very slow. Hence, even though lipids are in close contact with the recently formed α -tocopheryl radical, it is rather unlikely that in the usual in vivo conditions the hydrogen abstraction reaction from lipidic chains should occur. Thus, the α -tocopheryl radical will rather remain unmodified until a proper vitamin E regenerator reacts with it, transferring it a proton to form α -tocopherol.

In previous papers we studied for the first time the mechanism and kinetics of reactions between CoQ and the OH radical (theoretically and experimentally)¹⁶ and between CoQ and the OOH radical (only theoretically).¹⁷ In this last

* Corresponding author e-mail: corchado@unex.es.

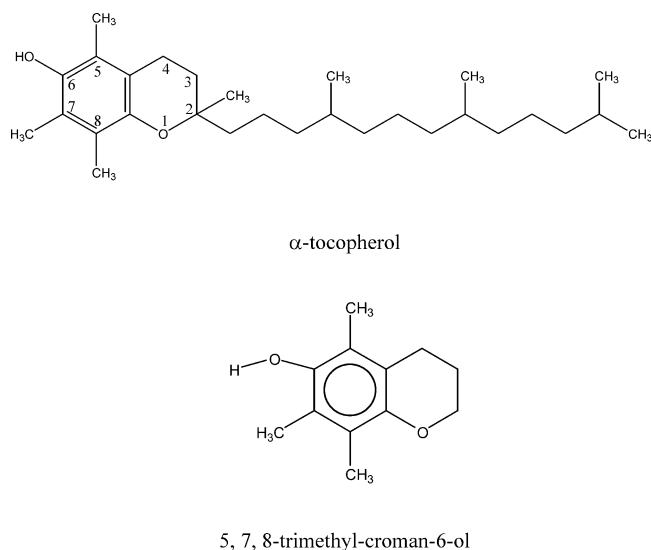


Figure 1. Numbering scheme for α -tocopherol and its model system employed in the present calculation.

case, directly related with the aim of the present work, we found that the OOH free radical attacks CoQ via two mechanisms: a hydrogen abstraction reaction from the phenolic hydrogen on the reduced form of CoQ (ubiquinol) and addition on the oxidized form (ubiquinone). We found that the reactivity of the OOH radical is dominated by the hydrogen abstraction reaction, with a rate constant of $5.3 \times 10^5 \text{ M}^{-1}\text{s}^{-1}$ at 298 K.

In the general context of the study of the antioxidant activity, and as a continuation of our previous studies with CoQ, in the present work we study the gas-phase reactivity of α -tocopherol with the hydroperoxy radical (HOO^\bullet) as a model of the reactions against oxidative stress that take place in biological systems without including environmental effects. The aim is 3-fold: first, to propose a mechanism to account for the attack of the hydroperoxy radical on α -tocopherol, i.e., to analyze theoretically the possible pathways; second, to obtain theoretical kinetics information; and third, to compare the antioxidant activity of the two potent natural radical scavengers, α -TOH and CoQ. In Section 2, we describe the theoretical methods and computational details used in the work; results and a discussion are given in Section 3; and conclusions are presented in Section 4.

2. Methods and Computational Details

Modeling. Because of the large size for our molecular system and the great number of calculations performed in the reaction path constructions, the real biological reaction was modeled in the following way. First, we replaced the trimethyltridecyl and methyl chains attached to carbon 2 in the α -tocopherol molecule by hydrogen atoms (see Figure 1). These chains have a prominent role in anchoring the tocopherol molecule to the membrane and restricting its mobility. However, it is very unlikely they have any major influence on the reactivity of the system, since the reactive part of tocopherols is the cromanol ring, which has been kept unchanged in our model system. Moreover, these chains are protected by the lipidic environment against attack from

cytosolic radicals; only part of the cromanol ring projects out from the membrane,³ and this is the only point where reactions with polar molecules solvated by cytosolic water can take place. Therefore, we modeled the α -tocopherol molecule by the 5,7,8-trimethylcroman-6-ol molecule (Figure 1). A similar model reducing the size of the real system had already been used with success in our previous studies of CoQ,^{16,17} and it was consistent with the conclusions of Foti et al.¹⁸ that the hydrogen abstraction reaction from CoQ is independent of the size of the chain attached to the aromatic ring.

Second, while the theoretical study was performed in the gas-phase, given the nonpolar character of the natural environment (lipid bilayer), one can reasonably assume that the conclusions will be roughly the same in both environments.

To study all the possible side reactions that can take place between α -tocopherol and the hydroperoxy radical, we took two mechanisms into account: the hydrogen abstraction reaction and the reaction of addition to the aromatic ring. With respect to the hydrogen abstraction mechanism, we considered that the hydroperoxy radical can abstract either the phenolic hydrogen (attached to the oxygen on carbon 6) or any of the methylic hydrogens (from the methyl groups attached to carbon atoms 5, 7, and 8). With respect to the addition reaction, we also take into account four addition centers, namely carbons 5, 6, 7, and 8. Therefore, we took eight possible reactions into account, four hydrogen abstraction reactions and four addition reactions, as shown in Figure 2.

Electronic Structure Calculations. The geometries of the reactants (α -TOH and $\cdot\text{OOH}$) and products (four abstraction products plus HOOH , as well as four addition products) were optimized using hybrid density functional theory (DFT) as implemented in the Gaussian 98¹⁹ suite of programs. Exchange and correlation were treated by the BHandHLYP method, which is based on Becke's half-and-half method²⁰ and the gradient-corrected correlation functional of Lee, Yang and Parr,²¹ using the 6-31G basis set.²² We will denote this level by its usual abbreviation:

- BHandHLYP/6-31G (hereafter called Level 0).

Vibrational frequencies were calculated using Level 0 in order to check that these geometries correspond to true minima on the potential energy surface, verifying that all the vibrational frequencies are real. Tables listing the geometries, energies, and vibrational frequencies of all the stationary points are given as Supporting Information. For the most favorable reaction channels (see Section 3) we located their saddle points and calculated reaction barrier heights using Level 0, checking the nature of the saddle points by verifying that they possess a single imaginary frequency. Starting from a saddle point, we followed the reaction path both toward reactants and products,²³ calculating vibrational frequencies after projecting out the motion along the reaction path using redundant internal coordinates.²⁴

When following the reaction path for the hydrogen abstraction reaction from the phenolic hydrogen, we found a minimum on the reactant side and another minimum on the product side. The two minima, which we will denote as

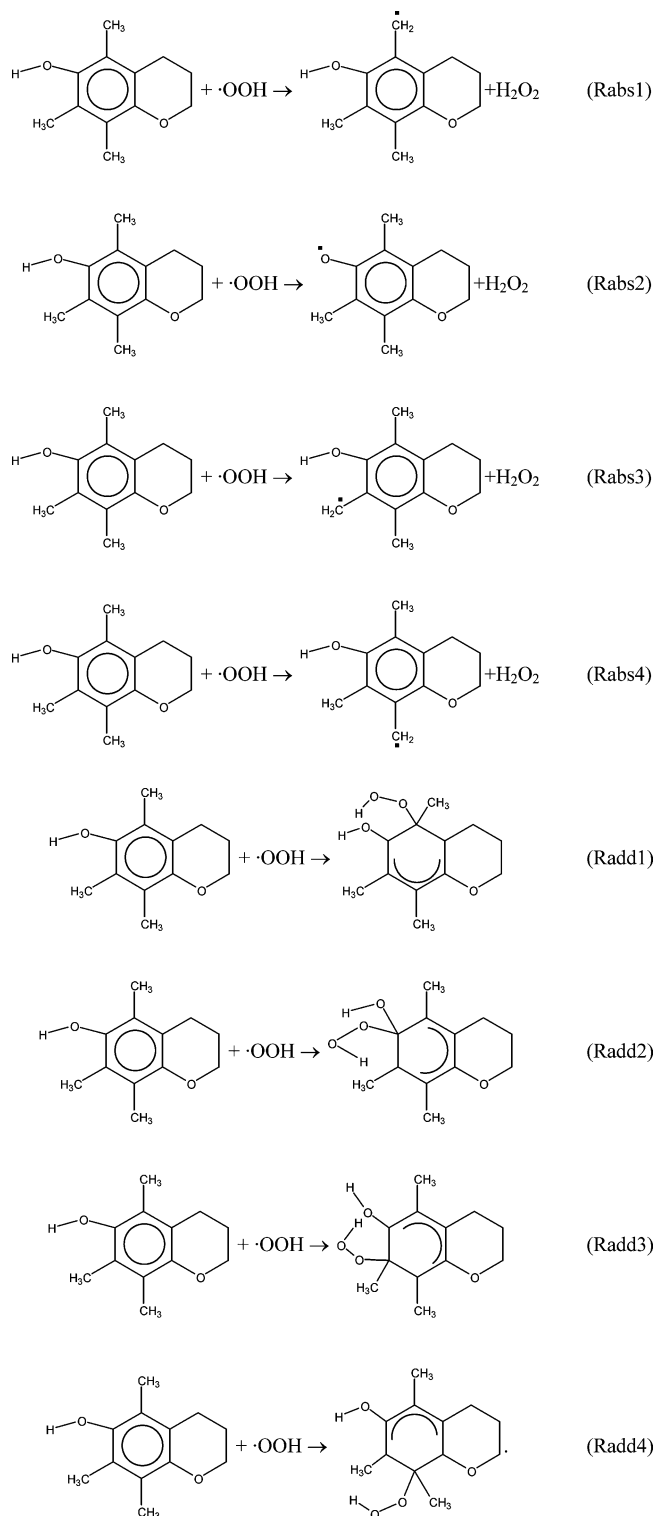


Figure 2. Reaction mechanisms taken into account for the α -tocopherol + $\cdot\text{OOH}$ reaction.

reactant well and product well, were further optimized and their vibrational frequencies were calculated using Level 0. Both were true minima (all the vibrational frequencies were real). Geometries, energies, and vibrational frequencies of the computed saddle points and complexes are also given as Supporting Information.

Dynamics Calculations. The kinetics study of the selected reaction mechanisms of α -tocopherol with the hydroperoxy radical were carried out using the direct dynamics approach,²⁵

by using the information on reaction paths described above and a mapping interpolation procedure,²⁶ in order to minimize the errors caused by the limited information we calculated. Rate constants were estimated using canonical variational transition state theory (CVT).²⁷ Quantum effects on motions transversal to the reaction path were included using quantum-mechanical vibrational partition functions in the harmonic oscillator approach, while quantum effects on the motion along the reaction path were included using a semiclassical multidimensional method for tunneling, namely the small-curvature tunneling method (SCT).²⁷ Kinetics calculations were performed using the Polyrate²⁸ and Gaussrate²⁹ computer codes.

It has been found that DFT methods usually underestimate barrier heights for hydrogen abstraction reactions, and an alternative DFT method has been devised for the accurate description of these barrier heights, denoted MPW1K.³⁰ Moreover, it is clear that the results also depend on the basis set employed in the calculations. To check the accuracy of our calculations, we performed selected single-point calculations using both BHandHLYP and MPW1K functionals and several extended basis sets, namely 6-311G(2d,p),³¹ 6-311+G(d,p),³¹ 6-311G+(2d,p),³¹ and MG3.³² These single-point calculations will be denoted by the usual double-slash notation:

- MPW1K/6-311G(2d,p)//Level 0 (hereafter called Level 1),
- BHandHLYP/6-311+G(d,p)//Level 0 (Level 2),
- BHandHLYP/6-311G(2d,p)//Level 0 (Level 3),
- BHandHLYP/6-311+G(2d,p)//Level 0 (Level 4),
- MPW1K/MG3//Level 0 (Level 5).

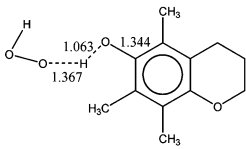
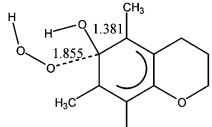
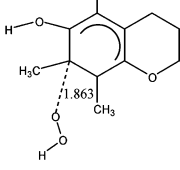
Using Level 1 we calculated single-point energies at selected points along the reaction path, while Levels 2 through 5 were used for single-point calculations only at the most relevant stationary points (reactants, products, and saddle point). This information was conveniently interpolated using the methods of ref 33 in order to perform dual-level kinetics calculations.³⁴ The dual-level kinetics calculations will be denoted using the recommended triple-slash notation, X//Y///Z, where the term to the right of the triple-slash, Z, denotes the lower level (Level 0), while the term to its left, X//Y, denotes the higher level (Levels 1 through 5).

3. Results and Discussion

Thermochemistry. As we noted in Section 2, we considered eight possible reactions: four abstraction reactions, namely Rabs1, Rabs2, Rabs3, and Rabs4, and four addition reactions, namely Radd1, Radd2, Radd3, and Radd4, as shown in Figure 2.

A priori, abstraction reactions seem to be more plausible, since addition reactions involve the breaking of the aromaticity of the system. Moreover, taking into account that the bond dissociation energies (BDE's) of C–H bonds are usually higher than those of phenolic O–H bonds,³⁵ from simple inspection of the products, chemical intuition leads us to predict that the most exothermic abstraction reaction will be Rabs2. Table 1 lists the calculated changes in the classical (Born–Oppenheimer) energy for the four abstrac-

Table 1. Energy Changes (in kcal/mol) for the Eight Reactions and Selected Saddle Points Calculated Using Level 0 (Distances are in Å)

Reaction	ΔE	Saddle point	ΔE^\ddagger
Rabs1	7.9		
Rabs2	-7.5		4.2
Rabs3	8.7		
Rabs4	8.2		
Radd1	8.9		
Radd2	5.5		6.8
Radd3	3.3		10.2
Radd4	6.7		

tion reactions. Only Rabs2 is an exoergic reaction. It can also be seen that Rabs1, Rabs3, and Rabs5 have similar endoergicities, which can be attributed to the fact that the bond being dissociated is the same (C–H bond) and their environments are quite similar. Since the differences in exoergicities between Rabs2 and the other abstraction reactions are greater than 15 kcal/mol, one can expect that the only significant abstraction reaction will be Rabs2, and this is the only abstraction reaction that we will study further. With respect to the addition reactions (Table 1), it seems that Radd2 and Radd3 are the most plausible reactions. Although they are endoergic, addition reactions sometimes show low activation energies, and in principle they could compete kinetically with the abstraction reaction Rabs2. Therefore we will continue with the study of Radd2 and Radd3 despite the differences in energy changes with respect to Rabs2 (more than 10 kcal/mol).

The geometry and energy (measured with respect to the reactants) of the saddle points along the most favorable reaction paths, namely, Rabs2, Radd2 and Radd3, are also listed in Table 1. It is also interesting to look at the changes of some geometrical features as the reactions proceed. Thus, in the addition reactions, the bonds being formed are significantly stretched at the saddle points for Radd2 and Radd3, being somewhat larger than a single C–O bond (1.435 Å in methanol, for example) and slightly shorter for Radd2, in agreement with the fact that this reaction shows a lower barrier if we assume that the reason is that the new bond is stronger. With respect to the abstraction reaction, the bond being broken is about 11% larger than in the

Table 2. Rate Constants and Transmission Coefficients for the Rabs2 and Radd2 Reactions (in $M^{-1} s^{-1}$) at Level 0

T (K)	Rabs2			Radd2		
	CVT	κ (SCT)	CVT·SCT	CVT	κ (SCT)	CVT·SCT
250	9.8(+03) ^a	9.1	8.9(+04)	3.0(−02)	0.9	2.7(−02)
275	1.9(+04)	6.4	1.2(+05)	1.3(−01)	0.9	1.2(−01)
298	3.1(+04)	4.9	1.5(+05)	4.3(−01)	0.9	3.7(−01)
300	3.2(+04)	4.8	1.5(+05)	4.7(−01)	0.9	4.1(−01)
325	5.1(+04)	3.8	2.0(+05)	1.4(+00)	0.8	1.2(+00)
350	7.8(+04)	3.1	2.5(+05)	3.6(+00)	0.8	3.0(+00)
400	1.6(+05)	2.4	3.8(+05)	1.7(+01)	0.8	1.4(+01)
500	4.7(+05)	1.6	7.6(+05)	1.7(+02)	0.8	1.4(+02)
600	1.0(+06)	1.3	1.4(+06)	8.3(+02)	0.3	6.9(+02)

^a 9.8(+03) stands for $9.8 \times 10^{+03}$.

reactants (1.063 versus 0.960 Å), while the bond being formed is 41% larger than in the products (1.367 versus 0.968 Å), i.e., the saddle point resembles reactants rather than products (it is an early transition state). Note also that the bond between carbon 6 and the phenolic oxygen is shortened. The reason is that the radical being formed is starting to take on part of the aromatic structure, and the C–O bond is starting to take on some double-bond character.

Kinetics. As the starting point in our kinetics studies, we located the saddle points along the reaction paths for the three selected reactions, namely Rabs2, Radd2, and Radd3 (Table 1). There are several features we would like to note. First, the reaction barrier is lower for the Rabs2 case. Second, the most endoergic reaction, Radd2, shows a lower barrier height than Radd3. Third, while the saddle point for Rabs2 maintains the aromaticity of the ring, the saddle points for Radd2 and Radd3 lose part of this aromaticity, as is manifested by a deviation of the planarity of the carbon to which OOH is being bonded with respect to the remaining carbons. The latter observation agrees with the fact that addition reactions show a higher barrier. Since Radd3 has a barrier about 3.5 kcal/mol higher than Radd2, in the rest of the paper we will consider that the only plausible path for an addition reaction is the addition to carbon 6, and therefore only take into account the competition between the abstraction Rabs2 and the addition Radd2 reactions.

After calculating the saddle points, we followed the reaction paths for both reactions and used this information to calculate the CVT rate constants and SCT transmission coefficients. The resulting CVT/SCT rate constants are listed in Table 2 for the temperature range 250–600 K, using Level 0. Several features merit discussion.

The rate constants for the abstraction reaction are several orders of magnitude greater than the rate constants for the addition reaction. Therefore, we can consider that the reaction between α -tocopherol and the hydroperoxy radical occurs exclusively by hydrogen abstraction of the phenolic hydrogen. There are three reasons why this is the only reaction that takes place. First, from an energy point of view, both the saddle point for the abstraction reaction and the products keep the aromaticity of the chromanol ring, while the addition reaction involves losing this aromaticity. Thus, the energy barrier against the reaction is about 2.5 kcal/mol lower for the abstraction case.

Table 3. Energy (ΔE) and Enthalpy (ΔH) at 298 K of Reaction (R) and Activation (\ddagger) for Rabs2 Using Different Levels of Calculation (in kcal mol⁻¹)

	ΔE_R	ΔH_R	ΔE^\ddagger	ΔH^\ddagger
Level 0	-7.7	-8.0	4.2	2.6
Level 1	-5.2	-5.5	6.3	4.7
Level 2	-7.3	-7.6	9.0	7.4
Level 3	-6.7	-7.0	8.5	6.8
Level 4	-6.9	-7.2	9.3	7.7
Level 5	-5.3	-5.6	7.5	5.9

Second, from an entropy point of view, the abstraction reaction is also favored. In both cases, as the reaction proceeds the relative motion of the two reactants is hindered, and some entropy is lost. However, in the abstraction reaction there is a cleavage of an O-H bond, while a new O-H bond is being formed. This leads to a larger amplitude motion of the hydrogen being transferred, increasing the entropy of this part of the system with respect to the reactants. This effect does not occur in the addition reaction, where there is a more subtle rearrangement of bonds and electronic structure, with a much smaller effect on the entropy of the system. Therefore, from an entropy point of view, the abstraction reaction is also favored. It can be analyzed quantitatively in a simple way by comparing the vibrational zero-point energies of the saddle points of the two reactions. Thus, while the zero-point energy of the saddle point of Rabbs2 is 175.5 kcal/mol, for Radd2 it is 178.3 kcal/mol, almost 3 kcal/mol higher.

Third, the transmission coefficient, which mostly takes into account quantum effects on the motion along the reaction path, increases the abstraction reaction by about a factor of 5 at 298 K, while it slightly diminishes the addition reaction.³⁸ This behavior was to be expected, since the abstraction reaction involves the motion of a light particle (a hydrogen atom) that can easily tunnel through the reaction barrier, while the addition reaction involves the movement of heavy atoms. In fact, at 298 K, about 80% of the abstraction reaction is due to tunneling.

Thus, the effective classical barrier height is expected to be around 6 kcal/mol lower for the abstraction reaction, and quantum effects are expected to lower this barrier much more than the addition reaction barrier. Addition can therefore not compete with abstraction.

These results agree with those obtained for the CoQ + OOH reaction,¹⁷ where the hydrogen abstraction reaction is also the dominant mechanism, although in that case only 50% of the reaction at 298 K is due to tunneling.

Influence of the Level of Calculation. The computational requirements for the thermochemical calculations of eight reactions and two converged rate constants for a system of this size are extremely high. This is why we selected a quite small basis set for our calculations (Level 0). Although it has been pointed out that DFT methods are not as sensitive as ab initio methods to the size of the basis set,⁴⁰ we decided to check the accuracy of our calculations against experimental values and higher-level calculations.

Table 3 lists the energy and enthalpy changes at 298 K of reaction and activation (estimated at the saddle point)

Table 4. Bond Dissociation Energies at 298 K and Enthalpy of the Rabbs2 Reaction Calculated Using Different Computational Levels (in kcal mol⁻¹)

	α -tocopherol	H ₂ O ₂	ΔH_R
Level 0	70.0	78.0	-8.0
Level 2	73.3	80.9	-7.6
Level 3	72.7	79.7	-7.0
Level 4	73.0	80.2	-7.2
Exp.	77.3 \pm 1.0 ^a	88.2 \pm 1.0 ^b	-10.9 \pm 2.0

^a Reference 36. ^b Reference 41.

calculated for Rabs2 using the different levels listed in Section 2. We shall begin by analyzing the reaction enthalpy. The experimental value of the enthalpy of reaction at 298 K as predicted by the differences in bond dissociation energies of the O-H bond in α -tocopherol (77.3 \pm 1.0 kcal/mol)³⁶ and hydrogen peroxide (88.2 \pm 1.0 kcal/mol)⁴¹ is -10.9 \pm 2.0 kcal/mol. Therefore, all of the methods predict a reaction less exothermic than the experimental reference values, Level 0 being the one that shows closest agreement taking into account the experimental error bar, and the MPW1K-based levels being the ones that deviate the most. The reason the smallest basis set gives the value closest to experiment is that errors in the bond dissociation energies compensate each other. Table 4 lists the BDE's of α -tocopherol and hydrogen peroxide computed using the BHandHLYP based levels. As one increases the basis set, both BDE's come closer to the experimental values, but the α -tocopherol BDE is improved more than the hydrogen peroxide BDE. As a result, increasing the basis set leads to poorer results, and Level 0 seems to give a more balanced description of the reaction. This seems to be a general behavior for these systems, because a similar result was found in our previous study of the CoQ + OOH reaction.¹⁷

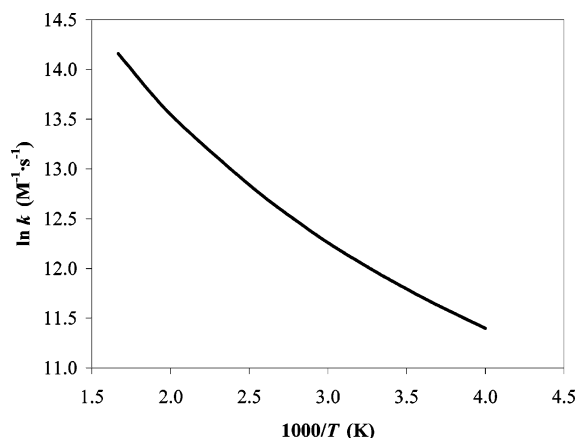
With respect to the barrier height, direct comparison with experimental or theoretical works is unfortunately not possible because such information is unavailable. We found that, leaving aside Level 0, the levels based on the MPW1K functionals (Levels 1 and 5) predict lower barrier heights than the BHandHLYP-based methods (Levels 2,3,4). In both cases, changes in the basis sets modify the computed magnitudes by about 1 kcal/mol for methods that use the same functional, confirming the conclusion of Koch and Holthausen⁴⁰ that DFT methods are fairly insensitive to the size of the basis set. In sum, Level 0 predicts the most exothermic reaction and the lowest barrier height, and based on its best agreement with the only experimental magnitude available, the enthalpy of reaction at 298 K, it will be the level of calculation used in the remainder of the paper.

To complete the check of the levels and basis sets, Table 5 lists the dual-level rate constants for Rabs2 at 298 K, using different functionals and basis sets. This table shows that increasing the level of calculation leads to a severe underestimate of the rate constant as compared with the value of the reaction between α -tocopherol and the *tert*-butylperoxyl radical in a nonpolar solvent, cyclopentane, which is the system closest to our reaction that has been measured experimentally.⁴² The reason is the higher barrier to the reaction predicted by higher-level methods, consistent with the fact that higher-level methods predict a less exothermic

Table 5. Dual-Level Rate Constants at 298 K for the Rabs2 Reaction (in $\text{M}^{-1} \text{s}^{-1}$)

	$k^{\text{CVT/SCT}}$
Level 0	$1.5(+05)^a$
Level 1///Level 0	$2.6(+03)$
Level 2///Level 0	$4.1(+02)$
Level 3///Level 0	$1.7(+02)$
Level 4///Level 0	$6.9(+01)$
Level 5///Level 0	$6.3(+02)$
Exp.	$2.6(+06)^b$
	$2.0(+05)^c$

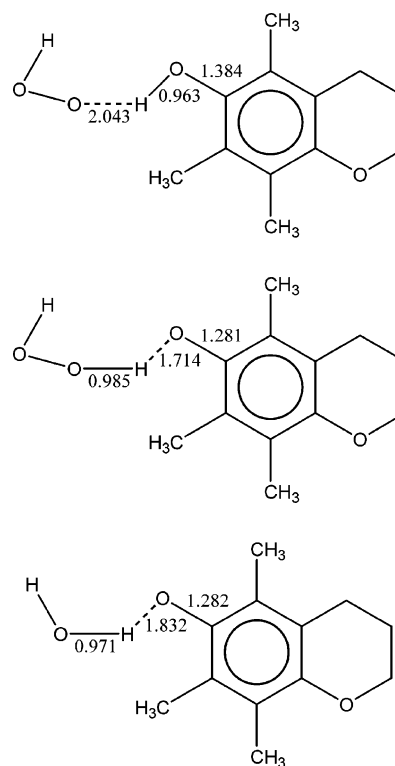
^a $1.5(+05)$ stands for $1.5 \times 10^{+05}$. ^b Reference 42, in cyclopentane solvent. ^c Reference 43, in water solvent.

**Figure 3.** Arrhenius plot of the rate constant for the α -tocopherol + $\cdot\text{OOH} \rightarrow \alpha$ -tocopheryl + H_2O_2 reaction at Level 0.

reaction. The modest Level 0 presents the best agreement with experiment, which is consistent with the behavior of this level in reproducing the experimental enthalpy of reaction at 298 K. However, the rate constant at 298 K is still lower than experiment, which leads us to think that the Level 0 barrier height is still slightly overestimated. However, since the system studied is different from the experimentally studied systems, it is not possible to know to which extent the Level 0 results are erroneous. In fact, changing the solvent leads to a decrease of the rate constant ($2.0 \times 10^{-5} \text{ M}^{-1} \text{ s}^{-1}$ in water,⁴³ for example). Therefore, we shall accept the Level 0 results as our best prediction for the gas-phase reaction between α -tocopherol and the hydroperoxy radical without further corrections to the theoretical method.

It is interesting to note that, although increasing the calculation level reduces the rate constant for Rabs2, no method predicts the Radd2 reaction to be competitive with Rabs2. Thus, as an example, the Level 1///Level 0 dual-level rate constants for Radd2 are 7 orders of magnitude lower than the Rabs2 rate constants calculated using the same level. Therefore, our conclusions hold no matter which level of calculation we use.

In brief, our best predictions for the overall rate constants are those given in Table 3 for the Rabs2 reaction, since Level 0 provides the best agreement with the available experimental measurements of the exothermicity and rate constants. These rate constants are shown in an Arrhenius plot in Figure 3. The curvature of the Arrhenius plot is an indication of the importance of tunneling. In fact at 298 K, about 80% of the

**Figure 4.** Geometry of the reactant well and product well for the α -TOH + $\cdot\text{OOH}$ reaction and the product well for the α -TOH + OH reaction (distances in Å).

reaction takes place by tunneling, rather than by classical over-the-barrier processes. A three-term Arrhenius fit to these data gave the expression

$$k(T) = 4.5 \times 10^{-2} T^{2.75} \exp(213/T)$$

for the rate constant in $\text{M}^{-1} \text{s}^{-1}$ in the interval 250–600 K. The activation energy can be obtained from the total rate constants through the usual definition

$$E_a(T) = R \frac{d(\ln k)}{d(1/T)}$$

with R being the gas constant, which is equivalent to determining the slope of the Arrhenius plot. At 298 K, our best estimate is 1.8 kcal/mol, very similar to our best estimate of 2.1 kcal/mol for the CoQ+OOH reaction.¹⁷

Intermediate Complexes. When following the Rabs2 reaction path at Level 0 starting from the saddle point and going downhill to reactants and products, we found that the reaction does not proceed directly but through the formation of two complexes. The first, that we will denote the *reactant well*, is a complex where the hydrogen bonded to the phenolic oxygen is weakly bonded to the oxygen in the hydroperoxy radical and is located on the reactant side of the reaction path (before the saddle point). The second, that will be denoted the *product well*, appears on the product side of the reaction path and shows that the hydrogen of the H_2O_2 product is bonded to the oxygen of the α -tocopheryl radical. The two wells are depicted in Figure 4. The energies and enthalpies of the reactant and product wells (measured with respect to reactants and products, respectively) are listed in Table 6.

Table 6. Energies and Enthalpies (at 298 K, in kcal mol⁻¹) of the Reactant Well and Product Well, Measured with Respect to Reactants and Products, Respectively

	reactant well		product well	
	ΔE	ΔH	ΔE	ΔH
Level 0	-4.6	-2.5	-11.7	-9.2
Level 1	-0.3	+1.8	-7.3	-4.8
Level 2	-3.3	-1.2	-9.2	-6.7

We have to note that the reactant complex is weakly bound, and its stability decreases as we increase the calculation level. This can be taken as an indication of the artificial stability afforded by the larger basis set superposition error of Level 0. Thus, the complex disappears when we include the thermal effects in using Level 1 energies, and its enthalpy stability is reduced to 1.3 kcal/mol with respect to reactants when we use Level 2 energies. Therefore, we can expect this well to have little influence on the mechanism of the reaction. However, the product complex is significantly more stable than the products. Even if we assume that Level 0 overestimates its stability due to the basis set superposition error, the complex is at least about 5 kcal/mol more stable than the products. Therefore, it might have some effect on the mechanism of the reaction.

In fact, the high stability of the product well can suggest that, after the reaction takes place, the H₂O₂ product remains bonded to the α -tocopheryl radical for a certain length of time. This is a positive effect for the cell. The partial protection provided by the H₂O₂ product to the most reactive center of the α -tocopheryl radical avoids or at least reduces its further attack on lipids in the membrane where it is anchored. In sum, this effect decreases the pro-oxidant action of the newly formed α -tocopheryl radical.

To check the stability of this complex, we also calculated the energy of a similar complex between water and the α -tocopheryl radical (Figure 4). Using Level 0 energies, this water- α -tocopheryl complex is 10.1 kcal/mol more stable than water and α -tocopheryl at infinite separation, and about 1.6 kcal/mol less stable than the complex between H₂O₂ and α -tocopheryl. Therefore, the H₂O₂ complex will have a longer life, hindering further reactions of the resulting radical better than cytosolic water. Thus, the presence of this complex could have a beneficial effect in avoiding the undesired pro-oxidant effect of α -tocopherol.

4. Concluding Remarks

There has been considerable experimental effort directed at understanding the role of antioxidants in biological processes and cell survival, in contrast with the paucity of theoretical studies. As a continuation of our previous studies on CoQ, we here studied the kinetics and dynamics of this antioxidant process using as a prototype reaction that of α -tocopherol with the hydroperoxy radical in the gas phase.

The hydroperoxy radical can attack α -tocopherol by two different pathways. We found that the most favorable mechanism is the hydrogen abstraction reaction from the phenolic hydrogen. This mechanism is favored by a lower transition state as a consequence of the fact that aromaticity

is conserved along the reaction path, as well as by a higher entropy of the transition state and a large probability of tunneling below the classical barrier. We found that this hydrogen abstraction reaction on α -tocopherol is responsible for the overall rate constant, $1.5 \times 10^5 \text{ M}^{-1} \text{ s}^{-1}$, with nearly 80% of the reactivity at 298 K being given by quantum-mechanical tunneling.

These results for α -TOH agree with the behavior observed for CoQ, where the rate constant at 298 K is $5.3 \times 10^5 \text{ M}^{-1} \text{ s}^{-1}$, and the tunneling contribution is about 50%. This similarity of the rate constants indicates that the two natural radical-trapping antioxidants provide similar antioxidant protection to the cell.

The most favorable abstraction reaction proceeds through two intermediates, one in the reactant channel with little or no influence on the dynamics of the reaction and another in the product channel. The high stabilization of the latter complex, formed by the H₂O₂ product bonded to the resulting α -tocopheryl radical, could hinder further reactions of the radical that can cause the observed pro-oxidant effects of α -tocopherol.

Acknowledgment. This work was partially supported by the Junta de Extremadura (Projects No. 2PR01A002 and 2PR03A075) and by the Dirección General de Investigación Científica y Técnica of Spain (Project BQU2003-04448)

Supporting Information Available: Cartesian coordinates, energies, and vibrational frequencies for the optimized stationary points computed at Level 0. This material is available free of charge via the Internet at <http://pubs.acs.org>.

References

- (1) (a) Niki, E. *Free Radical Res.* **2000**, *33*, 693–704. (b) Pryor, W. A. *Free Radical Biol. Med.* **2000**, *28*, 141–164.
- (2) Burton, G. W.; Ingold, K. U. *Acc. Chem. Res.* **1986**, *19*, 194–201.
- (3) Wang, X.; Quinn, P. J. *Prog. Lipid Res.* **1999**, *38*, 309–336.
- (4) Bowry, V. W.; Ingold, K. E. *Acc. Chem. Res.* **1999**, *32*, 27–34.
- (5) Niki, E. *Chem. Phys. Lipids* **1987**, *44*, 227–253.
- (6) For a recent review see Niki, E.; Nogichu, N. *Acc. Chem. Res.* **2004**, *37*, 45–51, and references therein.
- (7) Stocker, R. *Trends Biochem. Sci.* **1999**, *24*, 219–223.
- (8) Ernster, L.; Dallner, G. *Biochim. Biophys. Acta* **1995**, *1271*, 195–204.
- (9) Forsmark-Andrée, P.; Dallner, G.; Ernster, L. *Free Radical Biol. Med.* **1995**, *19*, 749–757.
- (10) Wolf, G. *Nutr. Rev.* **1997**, *55*, 376–378.
- (11) Barclay, L. R. C. *Can. J. Chem.* **1993**, *71*, 1–16.
- (12) Castle, L.; Perkins, M. J. *J. Am. Chem. Soc.* **1986**, *108*, 6381–6382.
- (13) Pryor, W. A.; Stickland, T.; Church, D. F. *J. Am. Chem. Soc.* **1988**, *110*, 2224–2229.

- (14) Valgimigli, L.; Banks, J. T.; Lusztyk, J.; Ingold, K. U. *J. Org. Chem.* **1999**, *64*, 3381–3383.
- (15) Bowry, V. W.; Stocker, R.; Walling, C. *Proc. Natl. Acad. Sci. U.S.A.* **1993**, *90*, 45–49.
- (16) Espinosa-García, J.; Gutierrez-Merino, C. *J. Phys. Chem. A* **2003**, *107*, 9712–9723.
- (17) Espinosa-García, J. *J. Am. Chem. Soc.* **2004**, *126*, 920–927.
- (18) Foti, M.; Ingold, K. U.; Lusztyk, J. *J. Am. Chem. Soc.* **1994**, *116*, 9440–9447.
- (19) Frisch, M. J.; Trucks, G. W.; Schlegel, H. B.; Scuseria, E.; Robb, M. A.; Cheeseman, J. R.; Zakrzewski, V. G.; Montgomery, J. A.; Stratman, R. E.; Burant, J. C.; Dapprich, S.; Millam, J. M.; Daniels, A. D.; Kudin, K. N.; Strain, M. C.; Farkas, O.; Tomasi, J.; Barone, V.; Cossi, M.; Cammi, R.; Menucci, B.; Pomelli, C.; Adamo, C.; Clifford, S.; Ochterski, J.; Pettersson, G. A.; Ayala, P. Y.; Cui, Q.; Morokuma, K.; Malick, D. K.; Rabuk, A. D.; Raghavachari, K.; Foresman, J. B.; Cioslowski, J.; Ortiz, J. V.; Stefanov, J. J.; Liu, G.; Liashenko, A.; Piskorz, P.; Komaromi, I.; Gomperts, R.; Martin, R. L.; Fox, D. J.; Keith, T.; Al-Laham, M. A.; Peng, C. Y.; Nanayakkara, A.; González, C.; Challacombe, M.; Gill, P. M. W.; Johnson, B. G.; Chen, W.; Wong, M. W.; Andres, J. L.; Head-Gordon, M.; Replogle, E. S.; Pople, J. A.; GAUSSIAN98 program, Revision A.7, Gaussian Inc., Pittsburgh, PA 1998.
- (20) Becke, A. D. *J. Chem. Phys.* **1993**, *98*, 1372–1377.
- (21) Lee, C.; Yang, W.; Parr, R. G. *Phys. Rev. B* **1988**, *37*, 785–789.
- (22) Hehre, W. J.; Ditchfield, R.; Pople, J. A. *J. Chem. Phys.* **1972**, *56*, 2257–2261.
- (23) Fast, P. L.; Truhlar, D. G. *J. Chem. Phys.* **1998**, *109*, 3721–3729.
- (24) Chuang, Y.-Y.; Truhlar, D. G. *J. Phys. Chem. A* **1998**, *102*, 242–247.
- (25) See, for example, Truhlar, D. G.; Gordon, M. S. *Science* **1990**, *249*, 491–498, and references therein.
- (26) Corchado, J. C.; Coitiño, E. L.; Chuang, Y.-Y.; Fast, P. L.; Truhlar, D. G. *J. Phys. Chem. A* **1998**, *102*, 2424–2438.
- (27) For a recent review on these methods see Truhlar, D. G.; Gao, J.; García-Viloca, M.; Alhambra, C.; Corchado, J. C.; Sánchez, M. L.; Poulsen, T. D. *Int. J. Quantum Chem.* **2004**, *100*, 1136–1152.
- (28) Corchado, J. C.; Chuang, Y.-Y.; Fast, P. L.; Villà, J.; Hu, W.-P.; Liu, Y.-P.; Lynch, G. C.; Nguyen, K. A.; Jackels, C. F.; Melissas, V. S.; Lynch, B. J.; Rossi, I.; Coitiño, E. L.; Fernandez-Ramos, A.; Pu, J.; Albu, T. V.; Steckler, R.; Garrett, B. C.; Isaacson, A. D.; Truhlar, D. G. POLYRATE-version 9.0, University of Minnesota, Minneapolis, 2002.
- (29) Corchado, J. C.; Coitiño, E. L.; Chuang, Y.-Y.; Truhlar, D. G. GAUSSRATE-version 9.0, University of Minnesota, Minneapolis, 2002.
- (30) Lynch, B. J.; Fast, P. L.; Harris, M.; Truhlar, D. G. *J. Phys. Chem. A* **2000**, *104*, 4811–4815.
- (31) Hehre, W. J.; Radom, L.; Schleyer, P. v. R.; Pople, J. A. *Ab initio Molecular Orbital Theory*, Wiley: New York, 1987.
- (32) Fast, P. L.; Sánchez, M. L.; Truhlar, D. G. *Chem. Phys. Lett.* **1999**, *306*, 407–410.
- (33) Chuang, Y.-Y.; Corchado, J. C.; Truhlar, D. G. *J. Phys. Chem. A* **1999**, *103*, 1140–1149.
- (34) Corchado, J. C.; Espinosa-García, J.; Hu, W.-P.; Rossi, I.; Truhlar, D. G. *J. Phys. Chem.* **1995**, *99*, 687–694.
- (35) As an example, Wayner et al. (ref 36) list an O–H bond dissociation energy for α -tocopherol of 77.3 kcal/mol, while Berkowitz et al. (ref 37) give a C–H bond dissociation energy in toluene of 88.5 kcal/mol.
- (36) Wayner, D. D. M.; Lusztyk, E.; Ingold, K. U.; Mulder, P. J. *Org. Chem.* **1996**, *61*, 6430–6433.
- (37) Berkowitz, J.; Ellison, G. B.; Gutman, D. *J. Phys. Chem.* **1994**, *98*, 2744–2765.
- (38) Note that the transmission coefficient κ is not only a tunneling correction but also takes into account three effects: tunneling, which tends to make $\kappa > 1$, nonclassical reflection of trajectories that classically would overcome the barrier, which tends to make $\kappa < 1$; and a better treatment of the reaction threshold than the canonical variational transition state theory, which also makes $\kappa < 1$. The net effect in the abstraction reaction is $\kappa > 1$, while in the addition reaction it is $\kappa < 1$. For a detailed description of the calculation of transmission coefficients and threshold corrections see ref 39.
- (39) Truhlar, D. G.; Isaacson, A. D.; Garrett, B. C. In *Theory of Chemical Reaction Dynamics*, Vol. 4, Baer, M., Ed. CRC Press: Boca Raton, FL, 1985; pp 65–137.
- (40) Koch, W.; Holthausen, M. C. *A Chemist's Guide to Density Functional Theory*, 2nd edition. Wiley-VCH: Weinheim (Germany), 2000.
- (41) Shum, L. G. S.; Benson, S. W. *Int. J. Chem. Kinet.* **1983**, *15*, 323–339.
- (42) Burton, G. W.; Doba, T.; Gabe, E. J.; Hughes, L.; Lee, F. L.; Prasad, L.; Ingold, K. U. *J. Am. Chem. Soc.* **1985**, *107*, 7053–7065.
- (43) Arudi, R. L.; Sutherland, M. W.; Bielski, B. H. J. *Oxy Radicals and Their Scavenger Systems*, Vol. 1, Cohen, G.; Greenwald, R. A. Eds. Elsevier: Amsterdam (The Netherlands), 1983.

CT0498932